CORCON 2015

Methodologies for Estimating Soil Resistivity Using the Inline Inspection and Close Interval Survey Data at External Material Loss Sites

Pavan K. Shukla,[1] Andrew Nordquist,[1] Len J. Krissa,[2] and Robert Moody[3]
[1]Southwest Research Institute® San Antonio, Texas 78238, USA
E-mail: *pshukla@swri.org*

[2]Enbridge Pipelines Inc., 10201 Jasper Ave NW, Edmonton, Alberta,
T5J 3N7 Canada

[3]Spectra Energy, 5400 Westheimer Court, Houston, Texas, 77056, USA

ABSTRACT

Soil resistivity is an important parameter that affects cathodic protection (CP). Although NACE International (NACE) does not recommend any specific CP criteria to account for variation in soil resistivity, the current density required to protect steel structures buried underground increases with decreasing soil resistivity. For example, approximately 1–2 mA/m^2 are recommended to protect a holiday on a pipeline buried underground with soil resistivity of 0.5–5 Ω-m. Similarly, only 0.1–1 mA/m^2 is recommended to protect the holiday of pipes placed in soil with a resistivity range of 5–15 Ω-m. Because the current density delivered to the pipe is inversely proportional to the soil resistivity, it is important to delineate the soil resistivity effect on CP effectiveness. In ISO 15589-1, it is recommended that –750 mV$_{CSE}$ be used for the on- and off-potential criterion when the soil resistivity is in the range of 10^4 to 10^5 Ω-cm, and –650 mV$_{CSE}$ for the on- and off-potential criterion when the soil resistivity is greater than 10^5 Ω-cm. Soil resistivity generally is not measured during close interval surveys or during annual CP surveys. Therefore, the soil resistivity data is not readily available. A methodology has been developed to estimate the soil resistivity using the inline inspection and close interval survey data. In additional, various techniques proposed in literature have also been evaluated. This paper describes the various methods used to estimate the soil resistivity and compares the estimates produced by these methods with field data.

Keywords: soil resistivity; cathodic protection; close interval survey; inline inspection.

NIGIS * CORCON 2015 * Nov 19 – 21, 2015 * Chennai

INTRODUCTION

Soil resistivity is an important parameter that affects cathodic protection (CP). Although NACE International (NACE) does not recommend any specific CP criteria to account for variation in soil resistivity, the current density required to protect steel structures buried underground increases with decreasing soil resistivity. For example, approximately 1–2 mA/m^2 are recommended to protect a holiday on a pipeline buried in soil with a resistivity of 0.5–5 Ω-m, and 2 mA/m^2 where the soil resistivity is 0.5 Ω-m.[1] Similarly, only 0.1-1 mA/m^2 is recommended to protect the holiday of pipes in soil with a resistivity range of 5–15 Ω-m.[1] Because the current density delivered to the pipe is inversely proportional to the soil resistivity, it is important to delineate the soil resistivity effect on CP criteria effectiveness. In ISO 15589-1,[2] it is recommended that -750 mV$_{CSE}$ be used for the on- and off-potential criterion when the soil resistivity is in the range of 100–1,000 Ω-m. In addition, the recommended value of on- and off-potential criterion is -650 mV$_{CSE}$ when the soil resistivity is above 1,000 Ω-m.

Soil resistivity generally is not measured during close interval or annual CP surveys. Therefore, resistivity data are not readily available. The work presented here is part of a larger project that involved evaluation of the NACE recommended CP criteria using field data: -850 mV$_{CSE}$ for the on- and off-potential criterion, and 100 mV polarization potential criterion.[3] The project included evaluating the CP criteria for a variety of soil and coating conditions. While the coating information was readily available, the soil resistivity data was not available for the entire coverage of the four pipelines. For this reason, three methods were used to estimate soil resistivity for four pipelines, designated as Pipelines A–D. The soil resistivity data was available for part of the length of Pipeline A and at two location of Pipeline D. Pipelines A and D soil resistivity data were used to check the soil resistivity estimates using the methods. This paper describes the methods used to estimate the soil resistivity, validated methods, and resistivity values obtained using the methods for Pipelines A–D.

SOIL RESISTIVITY ESTIMATION METHODS

The following three soil resistivity estimation methods were used in this work:

- Moghissi Method
- Yunovich Method
- Shukla-Nordquist Method

Moghissi Method: Moghissi et al. (2009)[4] presented a correlation analysis that related holiday size to soil resistivity near the holiday site and deviations in on- and off-potentials at the site. Specifically, Moghissi, et al. (2009) proposed the following correlation between the holiday (i.e., flaw) size and soil resistivity:

$$Flawsize = \frac{10^4 \cdot exp(0.000162 \cdot R_s)}{(0.843 - 0.02797 \cdot [DoC + VfD])}\left\{1 - \frac{IR_{dip}}{IR_{total}}\right\}^2 \tag{1}$$

where

$Flawsize$	—	Size of the holiday (cm^2)
R_s	—	Soil resistivity (Ω-m)
DoC	—	Depth of cover for pipeline (m)
VfD	—	Vertical distance of the flaw from 12 o'clock position (m)
IR_{dip}	—	Potential difference between the on- and off-potentials at the holiday site (V)
IR_{total}	—	Potential difference between the on- and off-potentials away from the holiday site (V)

A schematic description of variables IR_{dip} and IR_{total} is presented in Figure 1. Close Interval Survey (CIS) potential measurements are taken at regular intervals along the pipeline. At the external corrosion site, a dip in on- and off-potential is observed.
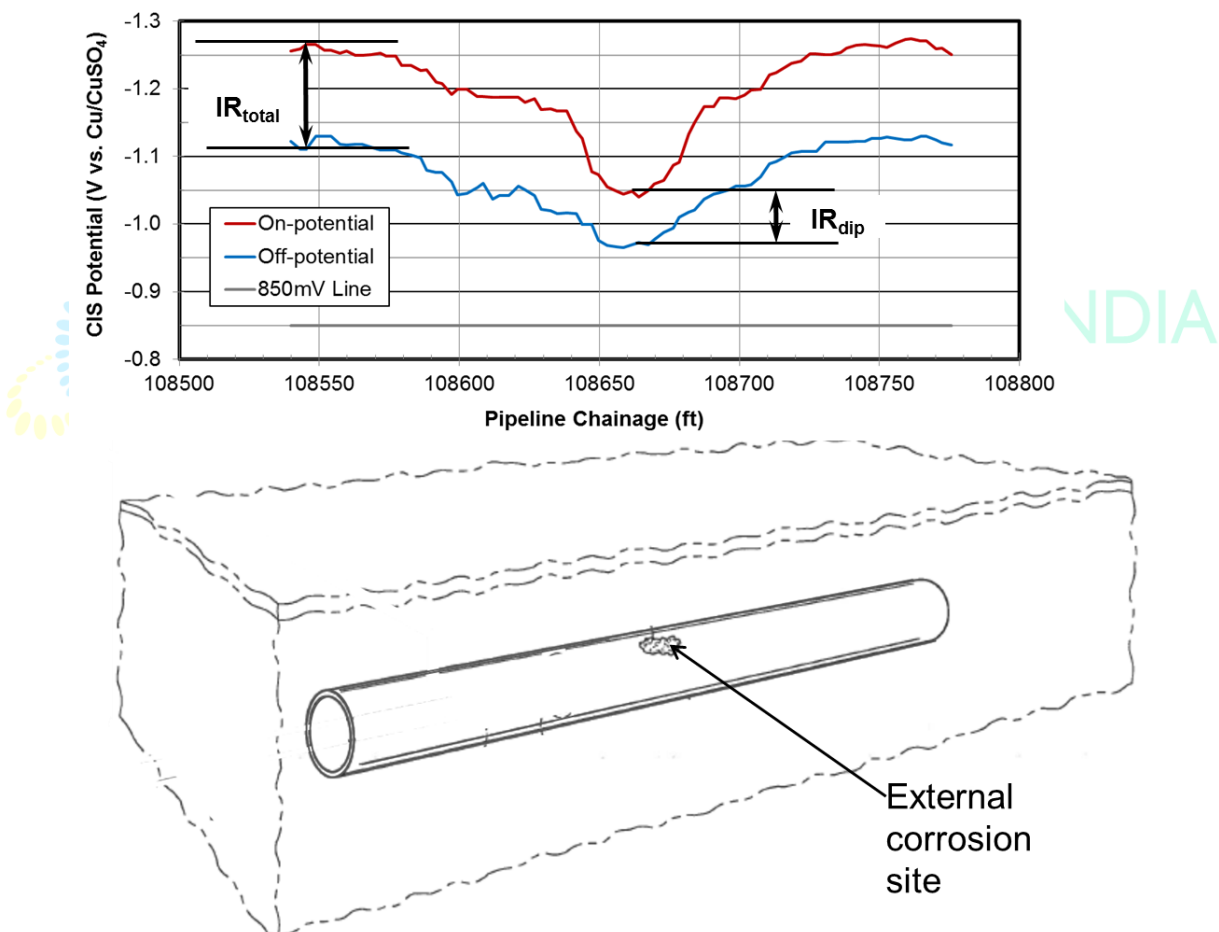
Figure 1. Schematic Description of IR_{dip} and IR_{total} in Equation 1.

As seen in Figure 1, IR_{dip} is the potential difference between the on- and off-potentials at the site and IR_{total} is the potential difference between the on- and off-potentials away from the site.

Eq. (1) is rearranged below to estimate the soil resistivity for given values of $Flawsize$, DoC, and the variables IR_{dip} and IR_{total}:

$$R_s = 6173 \left[\left(\frac{Flawsize \cdot (0.843 - 0.02797 \cdot [DoC + VfD])}{10^4 \cdot \left\{ 1 - \frac{IR_{dip}}{IR_{total}} \right\}^2} \right) - 1 \right] \qquad (2)$$

Yunovich Method: This method is obtained from the work by Yunovich et al. (2007)[5] where the author attempted to establish a numerical relationship between a pipeline coating flaw size (i.e., holiday size) and the electrical potential variation in the soil around it. Yunovich et al. (2007) did not provide a correlation between flaw size and other variables in equation form; instead, the author presented numerical studies on variations of pipeline coating flaw size (or holiday size) with soil resistivity, potential variation in the soil around the flaw, and depth of cover. The numerical studies presented by Yunovich et al. (2007) were in graphical form, and the data in the graphs were used in this work to develop a correlation similar to the one given by Eq. 1. Specifically, graphical data were extracted, a set of equations were fitted to the data, and equation coefficients were combined and normalized to develop the following correlation between the soil resistivity, depth of cover, and potential dip at the flaw site:
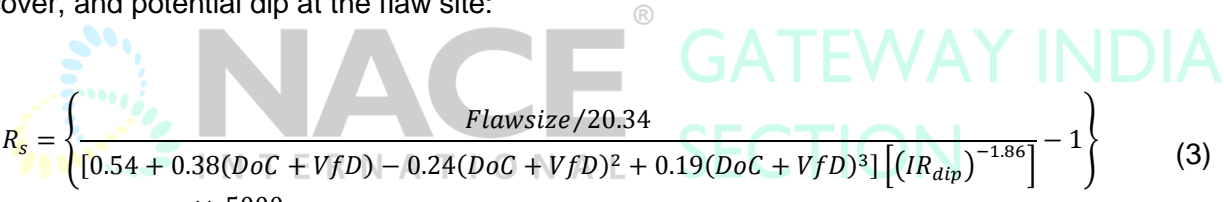
$$R_s = \left\{ \left(\frac{Flawsize/20.34}{[0.54 + 0.38(DoC + VfD) - 0.24(DoC + VfD)^2 + 0.19(DoC + VfD)^3] \left[(IR_{dip})^{-1.86} \right]} \right) - 1 \right\} \times 5000 \qquad (3)$$

Various variables in the above equation are the same as ones used in Eq. 1.

Shukla-Nordquist Method: This method is based on a combination of Ohm's Law, Faraday's Law, and Newman's Equation, which relates resistance to the charge flow on a holiday site to the soil resistivity and the holiday equivalent radius (Newman, 1966).[6] It is referred to as the Shukla-Nordquist Method for the sake of identification, based on their implementation of the relationship. Ohm's law is given by the following equation:

$$R = \frac{\Delta V}{iS} \qquad (4)$$

where

R	—	Resistance to the charge flow at the holiday site (Ω)
ΔV	—	Potential difference between current source and sink (V)
i	—	Corrosion current density at the holiday site (A/m^2)
S	—	Surface area of the holiday site (m^2)

NIGIS * CORCON 2015 * Nov 19 – 21, 2015 * Chennai

Faraday's Law relates corrosion current density at the holiday site to growth rate measured using inline inspection (ILI):

$$i = \frac{G_R nD}{100Ka} \tag{5}$$

where

G_R	—	Corrosion growth rate at the holiday sites (MPY)
n	—	Number of electrons per atom of iron in the iron oxidation reaction = 2
D	—	Density of pipeline grade carbon steel = 7.8 gm/cm^3
K	—	Constant of proportionality as specified in Fontana (Fontana, 1987)[7]
a	—	Molar weight of iron = 55.8 gm/mole

Finally, Newman's equation relating resistance R(ohms) with soil resistivity R_s(ohm-m) and surface of the holiday is given by the following:

$$R = \frac{R_s}{4}\sqrt{\frac{\pi}{S}} \tag{6}$$

The above three equations are combined to obtain the following equation, relating soil resistivity with other variables:

$$R_s = \frac{400Ka\Delta V}{G_R nD\sqrt{\pi S}} \tag{7}$$

Corrosion growth rates G_R and area of each external corrosion site S are available in the ILI data for all four pipelines. In Eq. 7, n, D, and K are known and are specified above. ΔV at each site is determined in the following way. ΔV is the electrical potential difference between source and sink. In the case of an external material loss (EML) site, the source potential is the off-potential at the site, and the sink potential is the highest off-potential near the site. The difference between the two provides the value of ΔV for the site. A schematic description of ΔV is presented in Figure 2.

NIGIS * CORCON 2015 * Nov 19 – 21, 2015 * Chennai
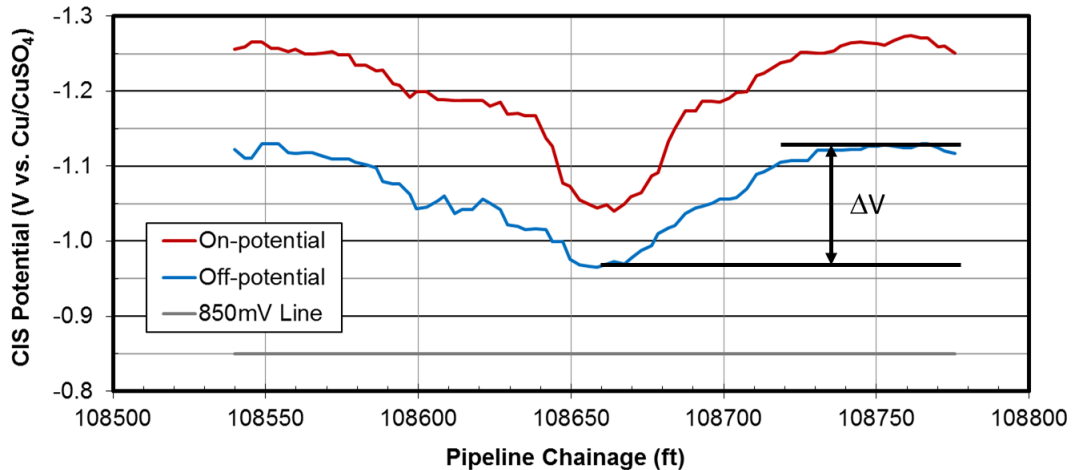
Figure 2. Schematic Description of ΔV in Eq. (7).

SOIL RESISTIVITY FIELD DATA

The soil resistivity field data were available for Pipelines A and D. The data are presented below.

Pipeline A Soil Resistivity Data: Pipeline A soil resistivity data were collected from three sources. Two of these included soil resistivity measurements during alternating current (AC) interference and mitigation surveys of the pipeline, and the third source was coupon survey data between Mileposts 190 to 290. Soil resistivity data were obtained during the AC interference and mitigation survey using the Wenner 4-Pin Method in accordance with ASTM G57.[8] The data source also indicated there were drought conditions when measurements were first taken and resistivity values in the range of 10k–2M Ω-m were recorded at a few locations. When a few months later after some rainfall the same locations were measured again, they showed values closer to 1,000 Ω-m. The Wenner 4-Pin Method provides average soil resistivity in a half-hemisphere, whose depth is equal to the pin separation. By varying the pin separation, soil resistivity tables versus depth were produced during the survey, with depths ranging from 2.5 ft. to 100 ft. Because typical depth of cover for Pipeline A ranges between 5 and 6 ft., measured soil resistivity values were obtained at each location by averaging soil resistivity data points from 5 ft. and 7.5 ft. depths. Additional soil resistivity data were acquired from coupon test data and rounded to the nearest 10 Ω-m. There is no specific detail provided with the coupon data regarding the measurement method used. The soil resistivity data from all three sources are presented in Figure 3, where three different legends denote the three sources of data. The data from the coupons overlap with the AC interference and mitigation survey "R" data in the middle of the pipeline (i.e., between 200–300 miles in the pipeline distance axis). This indicates that coupon, AC interference, and mitigation survey "R" datasets are sufficiently reliable to be used in this work. The AC interference and mitigation survey "C" soil resistivity data, denoted by red squares, cover up to the first 150 miles in the pipeline distance axis. As seen in the figure, some soil resistivity values based on AC interference and mitigation survey "C" are extremely high and overlap between the two AC sources is minimal. In fact, it appears the "C" source data is an order of magnitude greater than the "R" source data, where they do overlap.

NIGIS * CORCON 2015 * Nov 19 – 21, 2015 * Chennai
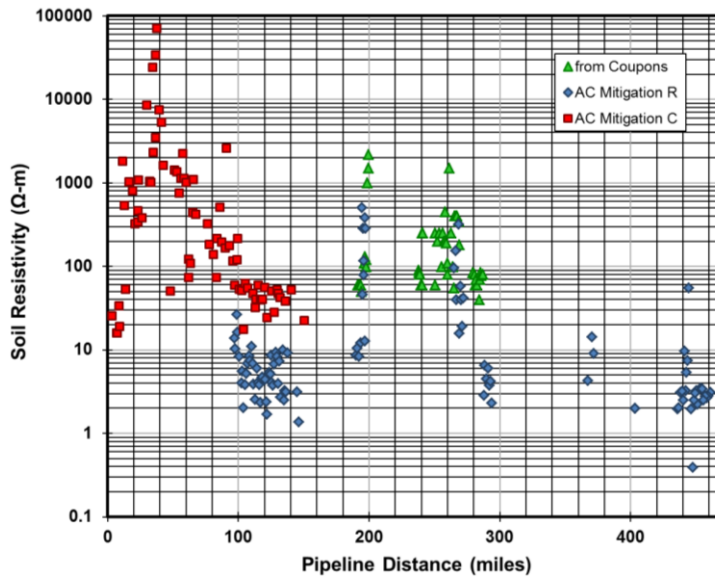
Figure 1. Measured Soil Resistivity Data for Pipeline A.

Pipeline D Soil Resistivity Data: Soil resistivity data for Pipeline D were available at two different locations. Measurements were made at the two locations, with three depths at each location, using the Wenner 4-Pin Method. The depths and resistivity values are shown in Table 1, while the data are presented in Figure 4. As seen in the data, the pipeline is characterized by an extremely low soil resistivity environment. This could be because the pipeline is located near the coast, where saline coastal water frequently enters the pipeline right of way.

Table 1. Measured Soil Resistivity With Depth for Pipeline D		
Milepost (mile)	**Depth (ft)**	**Resistivity (Ohm-m)**
125.88	5	0.48
125.88	10	0.39
125.88	20	4.60
176.02	5	7.46
176.02	10	5.74
176.02	20	6.51
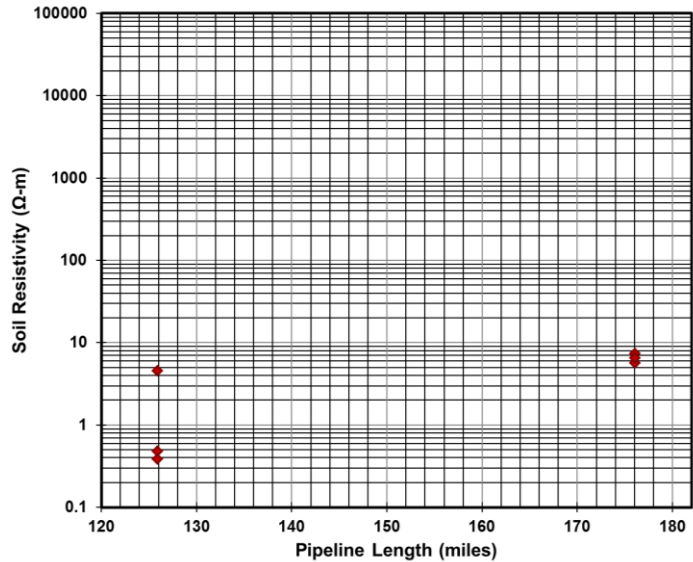
Figure 2. Measured Soil Resistivity Data for Pipeline D.

SOIL RESISTIVITY ESTIMATES AND COMPARISON WITH FIELD DATA

Various parameter values for soil resistivity estimates are provided. The depth of cover for Pipeline A is 5 ft. The other parameters used to estimate the soil resistivity profile for Pipeline A are presented in Figure 5.

| (a) | (b) |
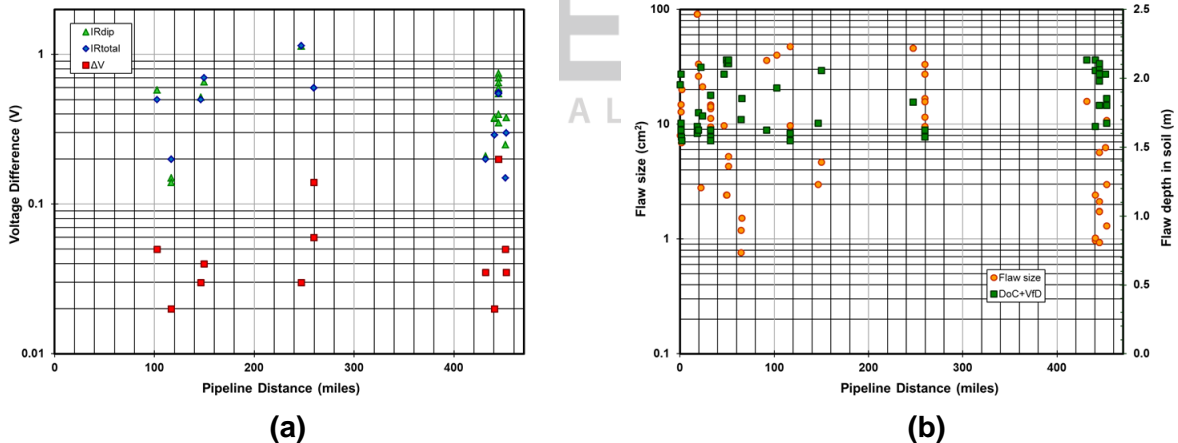
Figure 1. Graphical Presentation of Parameters Used to Estimate Soil Resistivity at EML Sites for Pipeline A. (a) Various Voltage Difference Parameters. (b) Flaw Size and Depth.

Measured versus estimated soil resistivities for Pipeline A are presented in Figure 6. The three methods rely on a change in the on- and off-potentials near the EML site. Such features in the on- and off-potentials only are available at EML sites. Because a dip in the on- and off-potentials was not observed in all cases even at EML sites, the estimated soil resistivity data are much sparser compared to the measured data for Pipeline A in Figure 6. Soil resistivity estimates using the Shukla-Nordquist method are closer to the measured data (Figure 6).
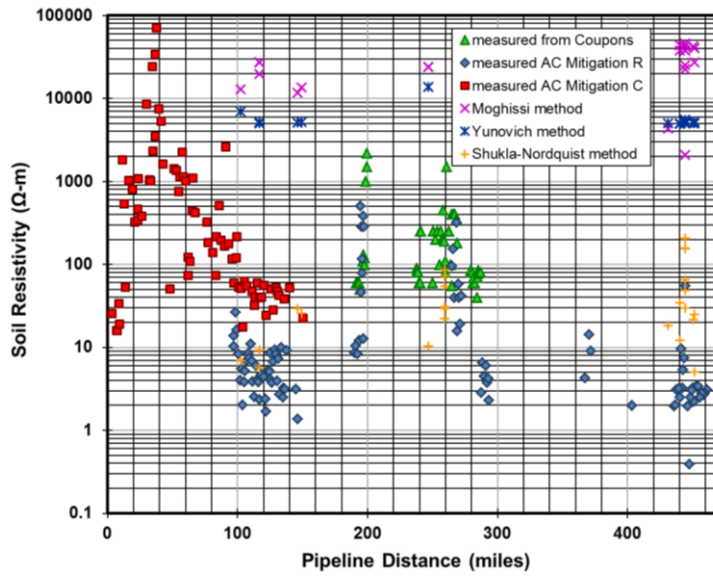
Figure 2. Measured Soil Resistivity Data for Pipeline A.

For Pipeline B, no soil resistivity field data are available. The depth of cover is assumed to be 5 ft. Various other parameters used for estimating soil resistivity profile for Pipeline B are provided in Figure 7. The estimated soil resistivity values for Pipeline B are presented in Figure 8.

(a)

(b)
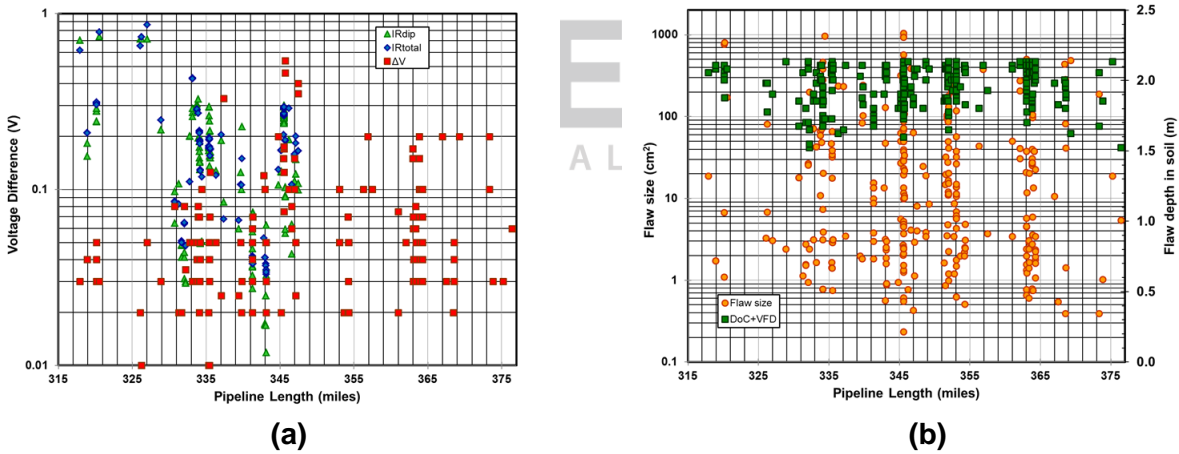
Figure 3. Graphical Presentation of Parameters Used to Estimate Soil Resistivity at EML Sites for Pipeline B. (a) Various Voltage Difference Parameters. (b) Flaw Size and Depth.
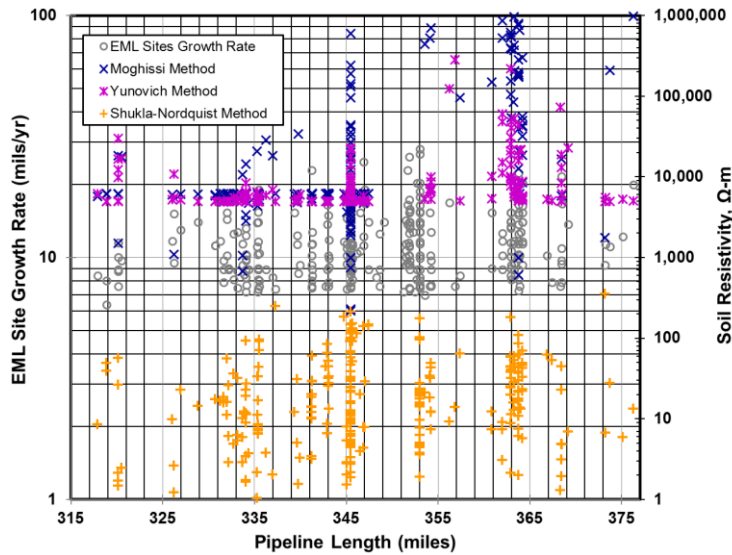
Figure 4. Soil Resistivity Estimates for Pipeline B.

For Pipeline C, no soil resistivity field data are available. The depth of cover is assumed to be 5 ft. Various other parameters used for estimating the soil resistivity profile are provided in Figure 9. The estimated soil resistivity values for Pipeline C are presented in Figure 10.

For Pipeline D, soil resistivity field data are available at two different locations. The depth of cover is assumed to be 5 ft. Various other parameters used for estimating soil resistivity for Pipeline C are provided in Figure 11. The estimated and measured soil resistivity values for Pipeline D are presented in Figure 12.

The estimated soil resistivity ranges using the three methods for the four pipelines are summarized in Table 2.
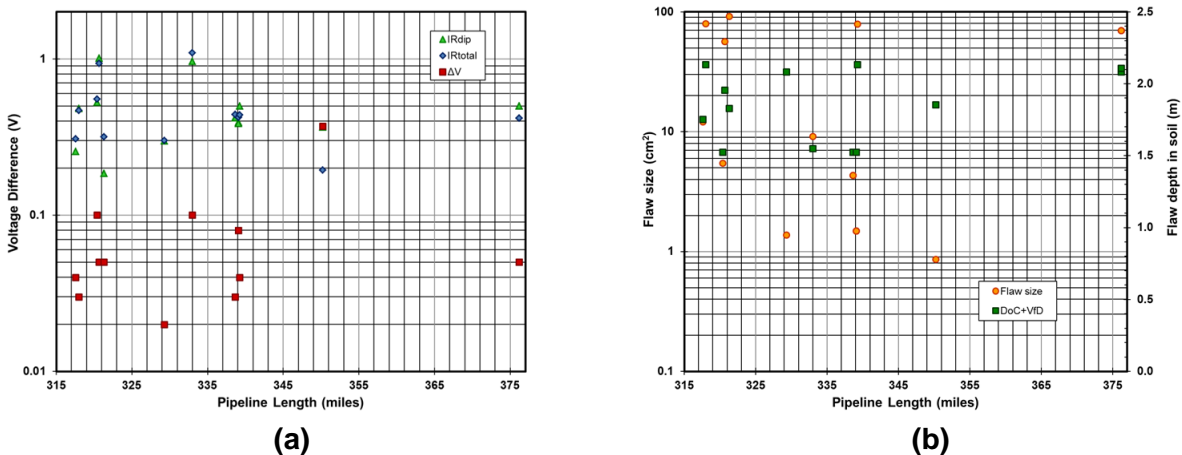
(a)

(b)

Figure 5. Graphical Presentation of Parameters Used to Estimate Soil Resistivity at EML Sites for Pipeline C. (a) Various Voltage Difference Parameters. (b) Flaw Size and Depth.
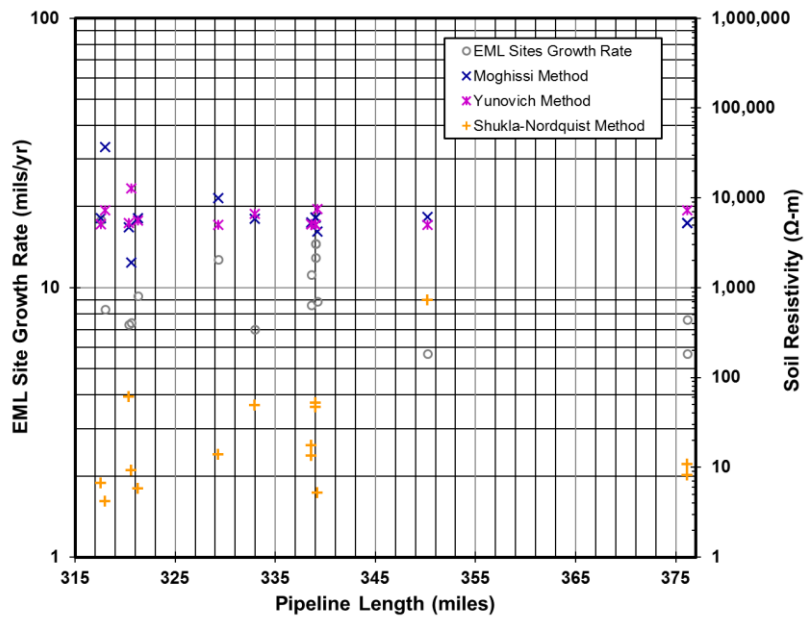
Figure 6. Soil Resistivity Estimates for Pipeline C.
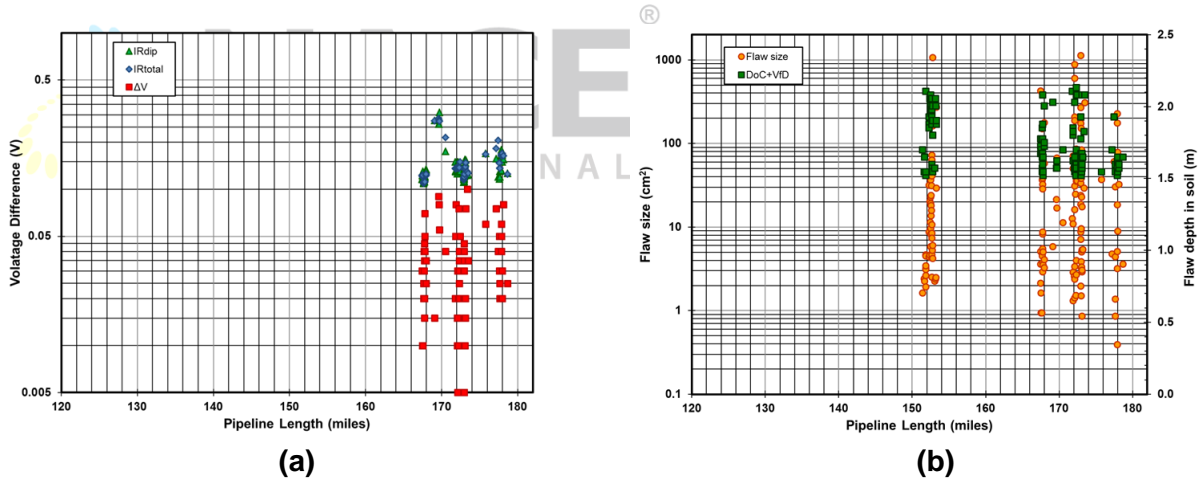
(a) **(b)**

Figure 7. Graphical Presentation of Parameters Used to Estimate Soil Resistivity at EML Sites for Pipeline D. (a) Various Voltage Difference Parameters. (b) Flaw Size and Depth.
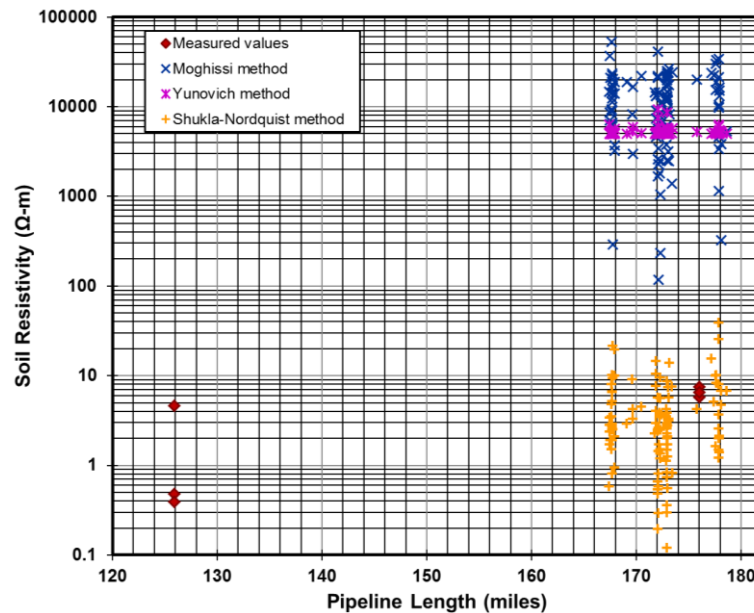
Figure 8. Measured Soil Resistivity Data for Pipeline D.

Table 1. Estimated Soil Resistivity (Ω-m) Range for Different Estimation Methods.			
Line	Moghissi Method	Yunovich Method	Shukla-Nordquist Method
Pipeline A	3410 to 8705	4976 to 13842	5.0 to 206.7
Pipeline B	218 to 1.41×10^{11}	4957 to 3.1×10^{6}	0.6 to 354.4
Pipeline C	1,909 to 37062	4975 to 12829	4.2 to 721.5
Pipeline D	118 to 416041	4960 to 10726	0.1 to 38.5

SUMMARY AND DISCUSSION

The Moghissi and Yunovich Methods provided unreasonably high soil resistivity estimates compared to field data. Therefore, an explanation is sought for estimates obtained by the Moghissi and Yunovich Methods. Moghissi et al. (2009) and Yunovich et al. (2007) used simulation results and statistical analyses of the simulation results to develop the correlations that relate flaw size to soil resistivity. In fact, Moghissi et al (2009) and Yunovich et al. (2007) were trying to predict flaw size using a set of parameters, with each parameter having its own range of values for which the models retain their validity. The result of each of their analyses—flaw size—also possesses a range of valid values.

Examination of Yunovich et al. (2007) indicates the valid range of flaw size is 300 to 400 cm^2. In the Moghissi Model, it is possible to use flaw sizes in the range from 0 to 650 cm^2; however, the model produces an inverse-squared relationship between soil resistivity and $1 - \frac{IR_{dip}}{IR_{total}}$, rendering it unstable when $\frac{IR_{dip}}{IR_{total}}$ approaches unity. It also is found that for a large fraction of EML sites in this work, $\frac{IR_{dip}}{IR_{total}}$ is close to unity. This is one plausible explanation for high soil resistivity estimates obtained from the Moghissi model.

NIGIS * CORCON 2015 * Nov 19 – 21, 2015 * Chennai

The relationship between flaw size and soil resistivity is further examined for its treatment in the Moghissi and Yunovich models. The Moghissi and Yunovich models provide an empirical relationship between flaw size and soil resistivity, and were developed using the simulation data. Furthermore, the Shukla-Nordquist model results match well with the field data (see Figures 6 and 12), whereas the Moghissi and Yunovich models overestimate soil resistivity values in all cases examined in the study. Based on this observation, the applicability of the flaw size range produced by the Moghissi and Yunovich models was examined using the following approach. The Moghissi and Yunovich model equations are provided in Eq. 1 and 3, respectively. The soil resistivity estimates from the Shukla-Nordquist model were used as input to the Moghissi and Yunovich model equations to predict the flaw sizes. Figure 13 shows measured flaw size distribution for pipelines included in the current study. Predicted versus actual flaw size is shown in Figure 14. Any deviation from the straight line in Figure 14 is an indication of the Moghissi and Yunovich models limitation. The Moghissi and Yunovich models behave well in the flaw size range of 400–1,000 cm^2.
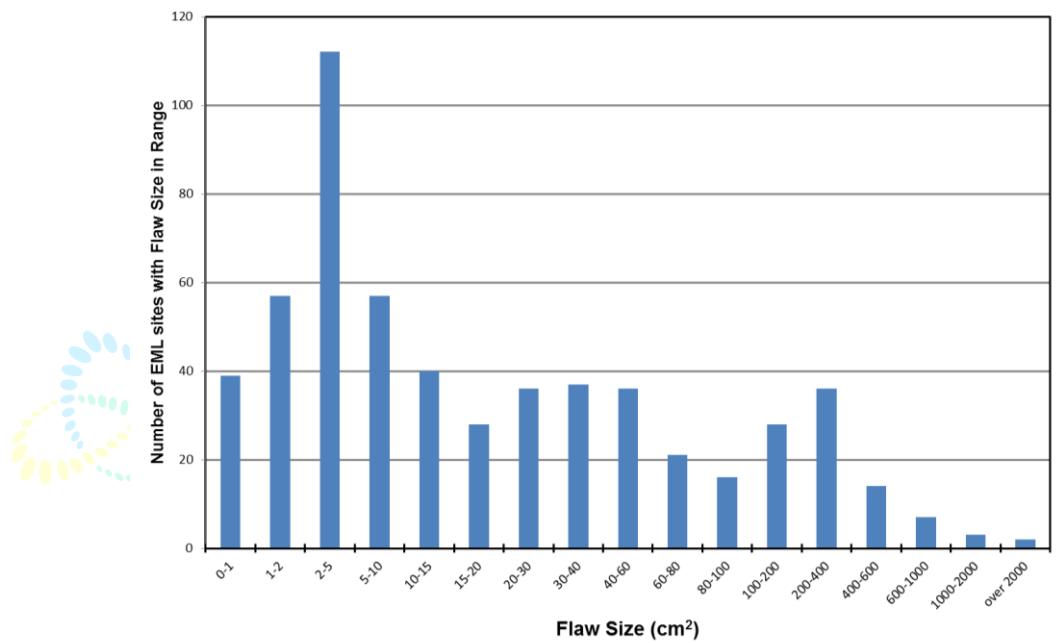
Figure 1. Distribution of Flaw Size for all Pipelines Included in This Study.
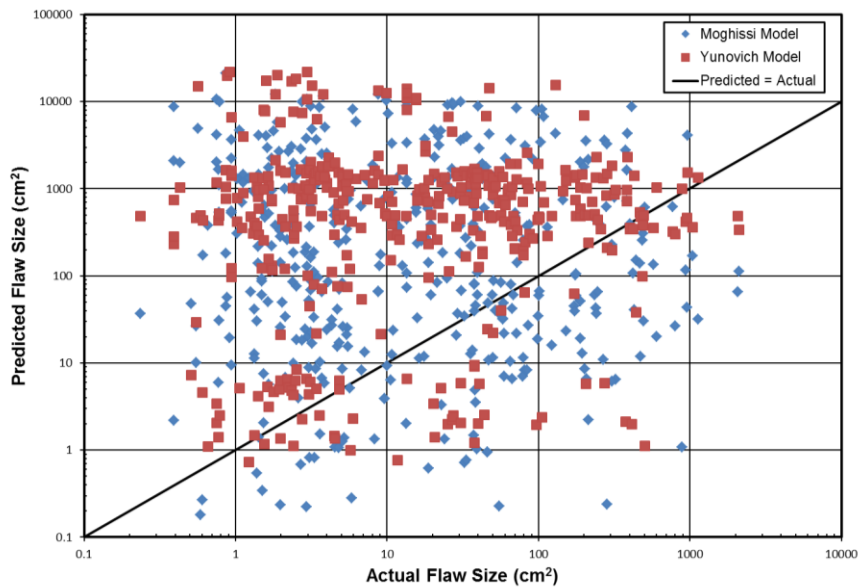
Figure 2. Predicted Versus Actual Flaw Size From the Moghissi and Yunovich Models.

A closer examination of Figure 14 shows there are some instances of good agreement between predicted and actual values, even at lower values of the flaw sizes. The fraction of sites lying on the linear curve, however, is small compared to the flaw size range of 400–1,000 cm^2.

Based on these results, it appears the Moghissi and Yunovich models are not suitable for estimating soil resistivity. Moreover, soil resistivity estimates produced by the Shukla-Nordquist model appear to be the most reasonable and within the range of the field data (see Figures 6 and 12). For example, in Figure 6, the measured soil resistivity range is 1 to 2,000 Ω-m (using AC Mitigation R and Coupon method), which bounds the Shukla-Nordquist model estimates, which are in the range of 5.0 to 206.7 Ω-m. The Shukla-Nordquist model was developed using first principles, whereas the Moghissi and Yunovich models were empirically developed using simulation data. This is one possible explanation for better model prediction using the Shukla-Nordquist model.

ACKNOWLEDGMENTS

REFERENCES

1. NACE International. NACE Corrosion Engineers Reference Book, 3rd Edition. Baboian, R. Ed. Houston, Texas: NACE International. 2002.

2. ISO 15589-1, "Petroleum and natural gas industries — Cathodic protection of pipeline transportation systems—Part 1: On-land pipelines." Geneva, Switzerland: International Standards. 2003.

NIGIS * CORCON 2015 * Nov 19 – 21, 2015 * Chennai

3. NACE International. "Control of External Corrosion on Underground or Submerged Metallic Piping Systems." Standard SP0169–2013. Houston, Texas: NACE International. 2013.

4. Moghissi O.C., J.P. McKinney, M.E. Orazem, and D. D'Zurko. "Predicting Coating Holiday Size Using ECDA Survey Data." CORROSION 2009. NACE International. Paper No. 09146. 2009.

5. Yunovich M. and S. Waters. "External Corrosion Direct Assessment for Unique Threats to Underground Pipelines." USDOT PHMSA Contract No. DTPH56-06-T-0012 Final Report. 2007.

6. Newman, J. "Resistance for Flow of Current to a Disk." *Journal of the Electrochemical Society*. Vol. 113, No. 5. pp. 501–502. 1966.

7. Fontana, M.G. Corrosion Engineering, 3rd edition. Singapore: McGraw-Hill Inc. 1987.

8. ASTM International. ASTM G57-12, "Standard Test Method for Field Measurement of Soil Resistivity Using the Wenner Four-Electrode Method." West Conshohocken, Pennsylvania: ASTM International. 2012.